

Evaluation of Engineering Stresses as the “Correct” Measure of “Physical” Stresses in Large Strain Geometrically Nonlinear Problems

A. E. Mohamed¹, N. M. Akasha², F. M. Adam³

¹Dept. of Civil Engineering, Sudan University of Science and Technology, Sudan

²Dept. of Civil Engineering, Sudan University of Science and Technology, Sudan

³Dept. of Civil Engineering, Jazan University, Kingdom of Saudi Arabia

Abstract: In this paper, Lagrangian formulations for geometric nonlinear plane stress/strain problems based on different stress measures are evaluated. A Total Lagrangian formulation based on the exact Engineering strains is developed. The 2ndPiola-Kirchhoff stresses based on the well known Green strains and the Engineering stresses based on the exact Engineering (geometric or conventional) strains obtained from Total Lagrangian formulations are compared with the true Cauchy stresses. The Engineering stresses based on the assumption of small shear strains are also compared with the above mentioned stresses. Geometric nonlinear Total Lagrangian formulations applied on two-dimensional elasticity using 4-node plane finite elements were used. The formulations were implemented into the finite element program (NUSAP). The solution of nonlinear equations was obtained by the Newton-Raphson method. The program was applied to obtain stresses for the different strain measures. The true Cauchy stresses were obtained by using the Logarithmic strains. The evaluation was based on comparing the results of three numerical examples. For moderate and large strains, the exact Engineering stresses are good measures of the correct physical stresses. Thus, these must be used when the stresses are required from a Total Lagrangian solution.

Keywords: Cauchy stresses, Engineering strain, Geometric Nonlinear, Plain stress/strain, Total Lagrangian

I. INTRODUCTION

Almost all structures behave in some nonlinear manner prior to reaching their limit of resistance. For this reason, most modern codes have incorporated certain provisions to consider nonlinear effects e.g. limit state design methods. Also, the use of light, high strength materials, resulting in light “tall” structures, introduces certain degrees of nonlinearity. This coupled with advance in solution methods and computing facilities make room for geometric nonlinear analysis. The major problem in geometrically nonlinear (GNL) finite element analysis is the need to define reference coordinates and to specify the relevant stress and strain measures.

The two main finite element formulations for GNL problems are the Eulerian formulations (EFMS) and the Lagrangian formulations (LFMS). As stated, among others, by Yang and Kuo [1], Crisfield [2], Zeinkiewicz and Taylor [3] and Mohamed [4] LFMS, in contrast to EFMS, are suitable in solid mechanics applications. This is mainly due to the ease with which they handle complicated boundaries and their ability to follow material points enabling the accurate treatment of history dependent materials. There are two main approaches to LFMS, namely the Total Lagrangian (TL) and the Updated Lagrangian (UL). Yang and Kuo [1], Zeinkiewicz and Taylor [3], Belytschko [5] and Marinkowic et al [6], stated that the UL approach provides the most efficient formulation and can be considered equivalent to the EFM. Wood and Zeinkiewicz [7] stated that the TL approach offers advantages since the initial configuration remains constant which simplifies formulation and computation. Surana and Sorem [8] presented a TL approach for framed structures with no restrictions on rotation increments. Djermane et al [9] pointed out that the TL formulation is now recognized as the most realistic civil engineering approach. But, the main serious drawback of the TL approach is that it is based on the Green strains, which are unsuitable for work with large strains. Also, the 2ndPiola-Kirchhoff stresses, which are work conjugate to the Green strains, are defined in the deformed configuration and should be transformed to the undeformed configuration [1], [2], [3], [4] and [8]. Thus, the TL approach while being very well established, having the above mentioned advantages and giving accurate displacement values, will result in stresses with no physical significance [2].

As for the definition of stress and strain measures, Crisfield [2] and Bonet and Wood [10] proposed the use, as work conjugate in the virtual work expression, the Green strains with the 2ndPiola-Kirchhoff stresses, the Engineering (conventional or geometric) strains with the Engineering stresses and the Logarithmic strains with the Cauchy “true” stresses. Yang and Kuo [1] used, as work conjugate, the Green-Lagrange strains with the 2ndPiola-Kirchhoff stresses, the Infinitesimal strains with the Cauchy stresses and the Updated Green strains with the Updated Kirchhoff stresses. They adopted the Updated Kirchhoff stresses as the measure of the “true”

physical stresses. In fact, the proposition that: using the UL approach converts the 2ndPiola-Kirchhoff stresses to the "true" stresses is also adopted by many researchers [2], [3], [5], [6] and [10].

An alternative TL approach that results in evaluating "correct" stresses was developed by Surana and Sorem [8]. Their formulation for framed structures removed the restrictions of small rotation increments by retaining nonlinear terms in the definition of the element displacement field. Mohamed [4] presented a TL formulation based on the Engineering strains which resulted in the correct stresses for small strain large rotation deformation of beams. Mohamed and Adam [11], [12] extended the TL formulation based on Engineering strains to the analysis of shell structures. Akasha [13] and Akasha and Mohamed [14], [15] developed a similar TL formulation for plane stress/strain problems. These formulations were based on using the Engineering strains with the Engineering stresses in the virtual work expression. The formulations were developed basing the variation of the Engineering strains on the variation of Green strains. These formulations are similar to the positional formulation based on Engineering strains used by Greco and Ferreira [16]. The formulations were, also, extended to include the evaluation of the true Cauchy stresses based on Logarithmic strains [13], [14] and [17]. The only limitation of these formulations is the assumption that the shear strains are small. However, it is possible to avoid this limitation by considering the exact variation of the Engineering strains.

This paper presents a TL formulation based the exact variation of Engineering strains. The paper is, also take an evaluation of the TL nonlinear stresses which are compared with the true Cauchy stresses presented by Akasha and Mohamed [17] using the Logarithmic strains. The comparison is carried out for plane stress/strain problems with the intention of investigating the effect of large strains on the different stress measures. The effect of avoiding the limitation on shear strains is, also, looked into. The comparison is considered as a criterion for ensuring the accuracy, consistency and convergence to the correct results of the nonlinear analysis. Thus, the aim of the evaluation is pointing out when the TL formulation based on Engineering strains is to be used, with confidence, in the analysis of large strain problems.

II. NONLINEAR FINITE ELEMENT FORMULATION

In the following sections there are two alternative Lagrangian formulations of the incremental equilibrium equations for large strain two dimensional problems which are outlined below.

2.1 Geometrically Non-linear Finite Element TL Formulation based on Green strains (TLG):

The 2ndPiola-Kirchhoff stresses, work conjugate to the Green-Lagrange strains, are the internal forces per unit initial area acting along the normal and tangential directions at the deformed configuration [1], [2] and [4]. Thus, these stresses are referred to the convected coordinates in the deformed configuration but measured per unit area of the undeformed body with attempts to take this into consideration in the virtual work expression result in an unsymmetrical stiffness matrix [4]. Hence, direct proportionality between the 2ndPiola-Kirchhoff stresses, s_0 , and the Green-Lagrange strains, e_0 , is assumed when writing the virtual work expression. In two dimensions, with reference to the initial configuration ($t=0$), the Green strains are given by:

$$\mathbf{e}_0 = \{e_x, e_y, e_{xy}\}^T = \frac{1}{2}(\mathbf{F}^T \mathbf{F} - [\mathbf{I}]) \quad (1)$$

where \mathbf{F} is the displacement gradient matrix.

In a finite element formulation equation (1) is written as:

$$\mathbf{e}_0 = \mathbf{e}_0^0 + \mathbf{e}_0^L = \mathbf{B}_0 \mathbf{a}_0 + \frac{1}{2} \mathbf{B}_L(\mathbf{a}_0) \mathbf{a}_0 \quad (2)$$

where \mathbf{a}_0 is the vector of nodal variables.

The nonlinear strain \mathbf{e}_0^L can be written as:

$$\mathbf{e}_0^L = \frac{1}{2} \mathbf{B}_L(\mathbf{a}_0) \mathbf{a}_0 = \frac{1}{2} \mathbf{A}_\theta \mathbf{G}_0 \mathbf{a}_0 \quad (3)$$

The strain displacement matrix \mathbf{B} is given by:

$$\mathbf{B} = \mathbf{B}_0 + \mathbf{B}_L(\mathbf{a}_0) \quad (4)$$

The tangent stiffness matrix now takes the form:

$$\mathbf{K}_T = \mathbf{K}_0 + \mathbf{K}_L(\mathbf{a}_0) + \mathbf{K}_\sigma \quad (5)$$

where:

$$\mathbf{K}_0 + \mathbf{K}_L(\mathbf{a}_0) = \int_{V_0} \mathbf{B}^T \mathbf{D} \mathbf{B} dV_0 \quad (6a)$$

in which \mathbf{D} is the modulus matrix, and the initial stress stiffness matrix is given by:

$$\mathbf{K}_\sigma = \int_{V_0} \mathbf{G}_0^T \mathbf{P}_{0i} \mathbf{G}_0 dV_0 \quad (6b)$$

in which \mathbf{P}_{0i} is the initial stress matrix.

The displacement increments $\Delta \mathbf{a}_0^i$ are evaluated by using \mathbf{K}_T and the residuals as:

$$\Delta \mathbf{a}_0^i = -\mathbf{K}_T^{-1} \boldsymbol{\phi}^i \quad (7)$$

The total displacements are, then, obtained as:

$$\mathbf{a}_0^{i+1} = \mathbf{a}_0^i + \Delta \mathbf{a}_0^i \quad (8)$$

The strain increments are defined by:

$$\Delta \mathbf{e}_0^i = \left[\mathbf{B}_0 + \mathbf{B}_L(\mathbf{a}_0^i) + \frac{1}{2} \mathbf{B}_L(\Delta \mathbf{a}_0^i) \right] \{ \Delta \mathbf{a}_0^i \} \quad (9)$$

And the stress increments are given by:

$$\Delta \mathbf{s}_0^i = \mathbf{D} \Delta \mathbf{e}_0^i \quad (10)$$

And the total stresses are:

$$\mathbf{s}_0^{i+1} = \mathbf{s}_0^i + \Delta \mathbf{s}_0^i \quad (11)$$

From which the nodal residual forces are evaluated as follows:

$$-\boldsymbol{\phi}^{i+1} = \mathbf{R} - \int_{V_0} \mathbf{B}^T \mathbf{s}_0^{i+1} dV_0 \quad (12)$$

where \mathbf{R} is the vector of applied equivalent nodal forces and:

$$\mathbf{B} = \mathbf{B}_0 + \mathbf{B}_L(\mathbf{a}_0^{i+1})$$

2.2 Geometrically Non-linear Finite Element TL Formulation based on Engineering strains (TLE):

In two dimensions the geometric strains, unit stretches, ε_x and ε_y are defined by the change in length per unit initial length of line elements originally oriented parallel to the x and y axes respectively. The shear strain γ_{xy} is the actual angle change.

The geometric strains, as defined above, are given in terms of Green strains by:

$$\begin{aligned} \varepsilon_x &= (g_x \cdot g_x)^{\frac{1}{2}} - 1 = (1 + 2e_x)^{\frac{1}{2}} - 1 \\ \varepsilon_y &= (g_y \cdot g_y)^{\frac{1}{2}} - 1 = (1 + 2e_y)^{\frac{1}{2}} - 1 \end{aligned} \quad (13)$$

And the shear strain is defined as:

$$\gamma_{xy} = \sin^{-1} \frac{e_{xy}}{(1 + 2e_x)^{\frac{1}{2}} (1 + 2e_y)^{\frac{1}{2}}} \quad (14)$$

where:

$$e_{xy} = g_x \cdot g_y = (1 + 2e_x)^{\frac{1}{2}} (1 + 2e_y)^{\frac{1}{2}} \sin \gamma_{xy}$$

$g_x = \frac{\partial R}{\partial x}$, $g_y = \frac{\partial R}{\partial y}$ are the displacement gradient vectors, and R is the position vector after deformation.

The variation in the Engineering strains is given by:

$$\delta \boldsymbol{\varepsilon}_0 = \mathbf{H} \delta \mathbf{e}_0 \quad (15)$$

where:

$$\begin{aligned} \delta \mathbf{e}_0 &= [\mathbf{B}_0 + \mathbf{B}_L(\mathbf{a}_0)] \delta \mathbf{a}_0 \\ &= [\mathbf{B}_0 + \mathbf{A}_\theta \mathbf{G}_0] \delta \mathbf{a}_0 = \mathbf{B} \delta \mathbf{a}_0 \end{aligned} \quad (16)$$

From which, the variations in the Engineering strains are given by:

$$\delta \boldsymbol{\varepsilon}_0 = \mathbf{H} \mathbf{B} \delta \mathbf{a}_0 = \mathbf{B}^* \delta \mathbf{a}_0 \quad (17)$$

In which \mathbf{B} is the strain matrix, and \mathbf{H} relates variation in Engineering strains to variation in Green strains.

The incremental equilibrium equations in terms of Engineering stresses are:

$$\mathbf{K}_T^* \Delta \mathbf{a}_0 = \mathbf{R} - \int_{V_0} \mathbf{B}^T \mathbf{H}^T \boldsymbol{\sigma} dV_0 = \mathbf{R} - \int_{V_0} \mathbf{B}^{*T} \boldsymbol{\sigma} dV_0 \quad (18)$$

where $\boldsymbol{\sigma}$ are the Engineering stresses.

The tangent stiffness matrix \mathbf{K}_T^* is now given by:

$$\mathbf{K}_T^* = \mathbf{K}_0^* + \mathbf{K}_L^* + \mathbf{K}_\sigma^* + \mathbf{K}_\sigma^{**} \quad (19)$$

where:

$$\mathbf{K}_0^* = \int_{V_0} \mathbf{B}_0^T \mathbf{H}^T \mathbf{D} \mathbf{H} \mathbf{B}_0 dV_0 \quad (20)a$$

and

$$\mathbf{K}_L^* = \int_{V_0} \mathbf{B}_0^T \mathbf{H}^T \mathbf{D} \mathbf{H} \mathbf{B}_L dV_0 + \int_{V_0} \mathbf{B}_L^T \mathbf{H}^T \mathbf{D} \mathbf{H} \mathbf{B}_0 dV_0 + \int_{V_0} \mathbf{B}_L^T \mathbf{H}^T \mathbf{D} \mathbf{H} \mathbf{B}_L dV_0 \quad (20)b$$

and \mathbf{K}_σ^* is the symmetric matrix dependent on the Engineering stress, and can be written as:

$$\mathbf{K}_\sigma^* = \int_{V_0} \mathbf{G}_0^T \mathbf{P}_{0i}^* \mathbf{G}_0 dV_0 \quad (21)$$

where \mathbf{G}_0 is a matrix containing shape function derivatives. and the initial stress matrix \mathbf{P}_{0i}^* is defined as:

$$\mathbf{P}_{0i}^* = \begin{bmatrix} \sigma_x^*[I] & \sigma_{xy}[I] \\ \sigma_{xy}[I] & \sigma_y^*[I] \end{bmatrix} \quad (22)$$

where $[I]$ is 2×2 unit matrix.

and $\boldsymbol{\sigma}^*$ is the stress vector given by:

$$\boldsymbol{\sigma}^* = \begin{Bmatrix} \sigma_x^* \\ \sigma_y^* \\ \sigma_{xy}^* \end{Bmatrix} = \mathbf{H}^T \begin{Bmatrix} \sigma_x \\ \sigma_y \\ \sigma_{xy} \end{Bmatrix} \quad (23)$$

and the additional geometric stiffness matrix \mathbf{K}_σ^{**} takes the following form:

$$\mathbf{K}_\sigma^{**} = \int_{V_0} \mathbf{B}^T \mathbf{P}_{0i}^{**} \mathbf{B} dV_0 \quad (24)$$

where \mathbf{P}_{0i}^{**} is obtained from:

$$\delta \mathbf{H}^T \boldsymbol{\sigma} = \mathbf{P}_{0i}^{**} \delta \boldsymbol{\varepsilon}_0 = \mathbf{P}_{0i}^{**} \mathbf{B} \delta \mathbf{a}_0 \quad (25)$$

Upon solving the incremental equilibrium equations for the displacement increments $\Delta \mathbf{a}_0^i$ and evaluating the total displacements a incremental strains are obtained as:

$$\Delta \boldsymbol{\varepsilon}_0^i = [\mathbf{H}] \left[\mathbf{B}_0 + \mathbf{B}_L(\mathbf{a}_0^i) + \frac{1}{2} \mathbf{B}_L(\Delta \mathbf{a}_0^i) \right] \{ \Delta \mathbf{a}_0^i \} \quad (26)$$

The stress increments are then given by:

$$\Delta \boldsymbol{\sigma}_0^i = \mathbf{D} \Delta \boldsymbol{\varepsilon}_0^i \quad (27)$$

And the total stresses are:

$$\boldsymbol{\sigma}_0^{i+1} = \boldsymbol{\sigma}_0^i + \Delta \boldsymbol{\sigma}_0^i \quad (28)$$

The residual forces, for a new displacement increment, are then equal to:

$$\begin{aligned} -\boldsymbol{\varphi}^{i+1} &= \mathbf{R} - \int_{V_0} \mathbf{B}^T \mathbf{H}^T \boldsymbol{\sigma}_0^{i+1} dV_0 \\ &= \mathbf{R} - \int_{V_0} \mathbf{B}^{*T} \boldsymbol{\sigma}_0^{i+1} dV_0 \end{aligned} \quad (29)$$

III. NUMERICAL RESULTS ANDDISCUSSION

The finite element TLG and TLE formulations described in the above section were implemented in the NUSAP coded by FORTRAN. Three numerical examples of large deformation problems were examined to demonstrate the degree of accuracy that can be obtained by using the geometrically non-linear formulations based on 4-node isoparametric plane stress/strain elements. The examples were also solved by using Green strains and the approximate Engineering strains [15]. The results of the stresses of the three TL formulations are compared with the true Cauchy stresses based on Logarithmic strains obtained using the formulation presented in references [13] and [17].

3.1 Cantilever under point load at free end:

The TLE (Eng Exact), approximate TLE (Eng) and TLG (Green) formulations were tested by analyzing the cantilever plate with vertical load at the free end. The cantilever is of dimensions $L=2.5 m$, $D = 1 m$ and $t = 0.1 m$ as shown in Figure (1). The numerical values of material property parameters are; Young's modulus, $E = 2 \times 10^8 kN/m^2$ and Poisson's ratio $\nu = 0.3$. The structure is modeled with 40 equal size isoparametric elements. The cantilever was, also, analyzed using Logarithmic (Log) strains for comparison.

Graphical comparison of results of the stresses at the support and at mid- span are presented in Figures (2) to (7). Tables (1), (2) and (3) show the stresses at mid-span. The results of the true Cauchy stresses are also shown. At mid-span the results for the direct stresses are almost identical for the Log and Eng exact formulations. The slight differences may be attributed to the large strain value at mid-span. The Green values vary greatly from the correct values and are almost zero in the x-direction for maximum load. The differences in the shear stress values are mainly due to the assumption that the shear strain is small in the formulations other than Eng Exact. The results for the direct stresses at the support are in close agreement. Those for the shear stresses at the support are in close agreement for Eng Exact and Log formulations. The shear values from the Eng formulation are approximate. The shear values from the Green formulation differ largely from the correct values as expected.

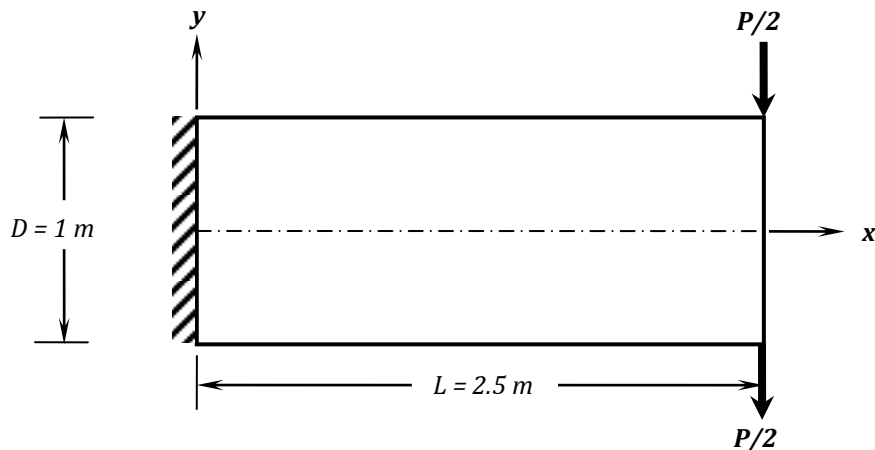


Fig. (1) Cantilever plate with vertical load at free end

Table (1): Average Nodal Stress in x-direction at mid span

LOAD (kN)	Stress (kN/m ²)				LOAD (kN)	Stress (kN/m ²)			
	Green	Eng	Log	Eng Exact		Green	Eng	Log	Eng Exact
0	0	0	0	0	92000	-5.64E+06	-5.84E+06	-6.63E+06	-4.86E+06
4000	-2.99E+05	-2.99E+05	-2.99E+05	-2.99E+05	100000	-5.82E+06	-5.83E+06	-6.65E+06	-4.51E+06
20000	-1.48E+06	-1.50E+06	-1.51E+06	-1.49E+06	116000	-5.89E+06	-5.09E+06	-5.70E+06	-2.82E+06
36000	-2.62E+06	-2.71E+06	-2.80E+06	-2.66E+06	132000	-5.47E+06	-3.03E+06	-2.79E+06	6.57E+05
52000	-3.69E+06	-3.89E+06	-4.14E+06	-3.75E+06	148000	-4.42E+06	8.10E+05	2.94E+06	6.54E+06
68000	-4.63E+06	-4.94E+06	-5.41E+06	-4.59E+06	164000	-2.62E+06	6.94E+06	1.24E+07	1.55E+07
84000	-5.37E+06	-5.67E+06	-6.38E+06	-4.95E+06	180000	8.12E+04	1.58E+07	2.63E+07	2.81E+07

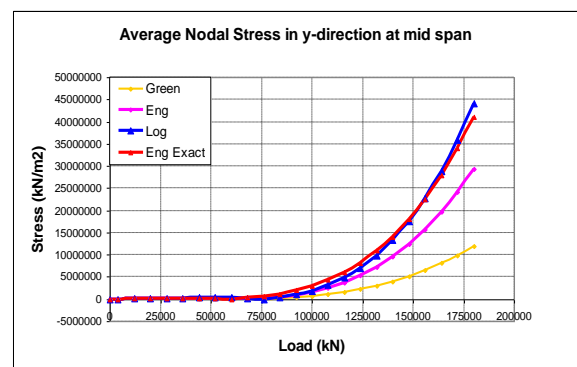
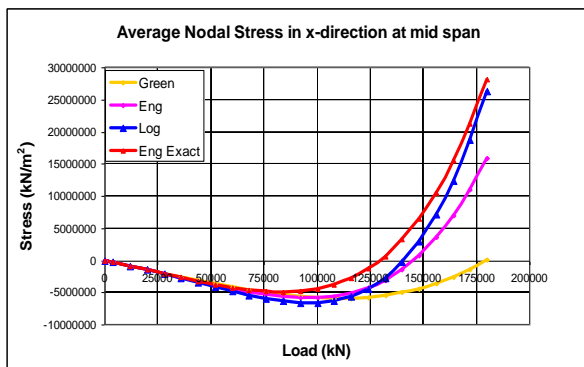


Fig. (2): Average Nodal Stress in x-direction at mid span Fig. (3): Average Nodal Stress in y-direction at mid span

Table (2): Average Nodal Stress in y-direction at mid span

LOAD (kN)	Stress (kN/m ²)				LOAD (kN)	Stress (kN/m ²)			
	Green	Eng	Log	Eng Exact		Green	Eng	Log	Eng Exact
0	0	0	0	0	92000	3.74E+05	9.81E+05	1.01E+06	1.99E+06
4000	2.42E+04	2.44E+04	2.44E+04	2.43E+04	100000	6.92E+05	1.68E+06	1.90E+06	3.02E+06
20000	1.20E+05	1.28E+05	1.38E+05	1.20E+05	116000	1.63E+06	3.81E+06	4.82E+06	6.08E+06
36000	1.98E+05	2.27E+05	2.77E+05	1.77E+05	132000	3.08E+06	7.24E+06	9.81E+06	1.09E+07
52000	2.22E+05	2.53E+05	3.65E+05	9.64E+04	148000	5.18E+06	1.24E+07	1.76E+07	1.80E+07
68000	1.35E+05	7.97E+04	2.34E+05	2.89E+05	164000	8.06E+06	1.96E+07	2.88E+07	2.79E+07
84000	1.39E+05	4.81E+05	3.91E+05	1.22E+06	180000	1.19E+07	2.93E+07	4.42E+07	4.11E+07

Table (3): Average Shear Stress at mid span

LOAD (kN)	Stress (kN/m ²)				LOAD (kN)	Stress (kN/m ²)			
	Green	Eng	Log	Eng Exact		Green	Eng	Log	Eng Exact
0	0	0	0	0	92000	-5.71E+05	-8.71E+05	-9.87E+05	-9.32E+05
4000	2.17E+04	-2.17E+04	-2.17E+04	-2.17E+04	100000	-6.48E+05	-1.05E+06	-1.22E+06	-1.12E+06
20000	-1.08E+05	-1.10E+05	-1.10E+05	-1.11E+05	116000	-8.31E+05	-1.48E+06	-1.83E+06	-1.54E+06
36000	-1.94E+05	-2.05E+05	-2.06E+05	-2.12E+05	132000	-1.06E+06	-1.99E+06	-2.53E+06	-1.98E+06
52000	-2.84E+05	-3.24E+05	-3.29E+05	-3.40E+05	148000	-1.35E+06	-2.48E+06	-3.08E+06	-2.25E+06
68000	-3.84E+05	-4.86E+05	-5.10E+05	-5.18E+05	164000	-1.72E+06	-2.73E+06	-2.90E+06	-2.06E+06
84000	-5.03E+05	-7.20E+05	-7.92E+05	-7.71E+05	180000	-2.17E+06	-2.42E+06	-1.07E+06	-9.74E+05

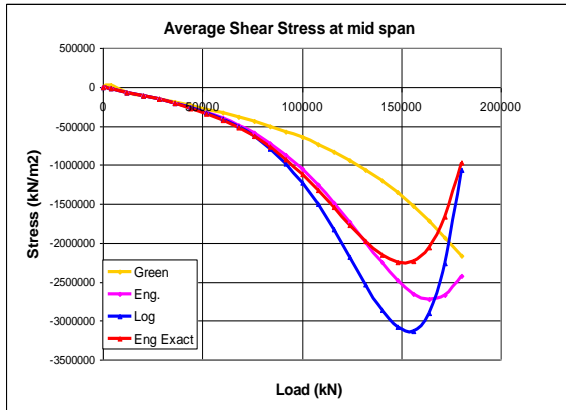


Fig. (4) Average shear stress at mid span Vertex

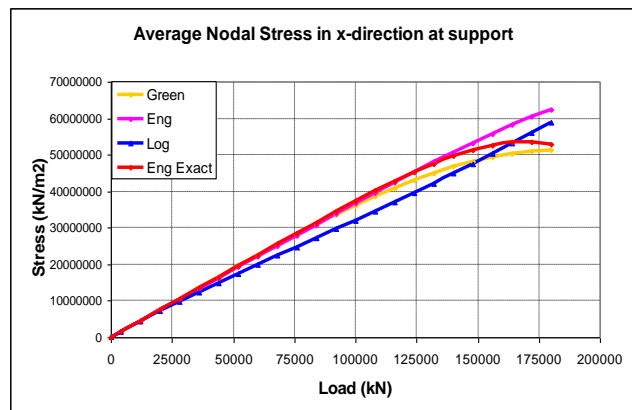


Fig. (5) Average Nodal Stress in x-direction at support

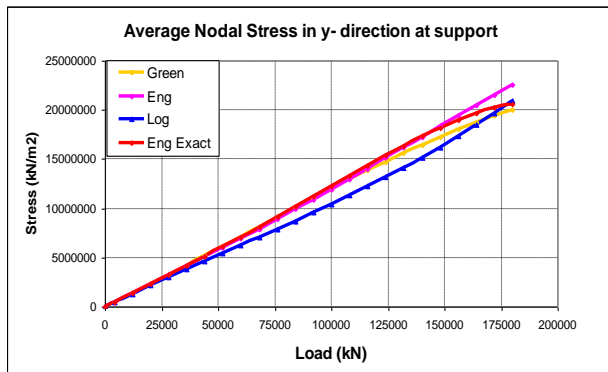


Fig. (6) Average Nodal Stress in y-direction at mid span

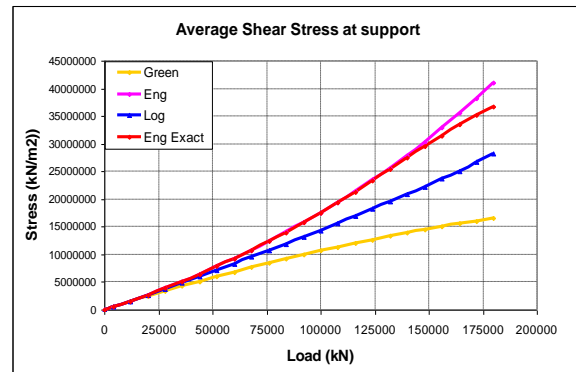


Fig. (7) Average shear stress at Support

3.2 Cantilever under pure bending at free end:

A cantilever subjected to pure moment is considered. The cantilever is of dimensions $L = 3000 \text{ mm}$, $D = 300 \text{ mm}$ and thickness $t = 60 \text{ mm}$ as shown in Figure (8). The numerical values of material property parameters are Young's modulus, $E = 210 \text{ GPa}$, and Poisson's ratio, $\nu = 0.3$. The structure is modeled with a mesh of 40-isoparametric elements. The mesh is of equal elements size of $150 \times 150 \text{ mm}$. The variations in the stresses at the support and at mid-span with load increments as computed by Eng exact formulation are compared with the Eng and Green formulations from Ref [15] and the Log formulation result presented in Ref [17]. The results are presented in Figures (9) to (14) and tables (4) to (9).

As can be seen from the tables the values of the stresses are generally small. The stresses in the x-direction are in close agreement for all formulations up to the 24000 N load. The Eng Exact and Log values clearly agree for all loads. There is a large difference between these values and the Green value for maximum load. The stresses in the y-direction and the shear stresses at mid-span show a similar trend with the Green values almost zero for all loads. This shows that the Engineering stresses, in contrast to the stresses obtained using Green strains, are correct measures of the physical stresses. The stresses at the support vary linearly and are all in close agreement. This is mainly due to the small strain values at the support.

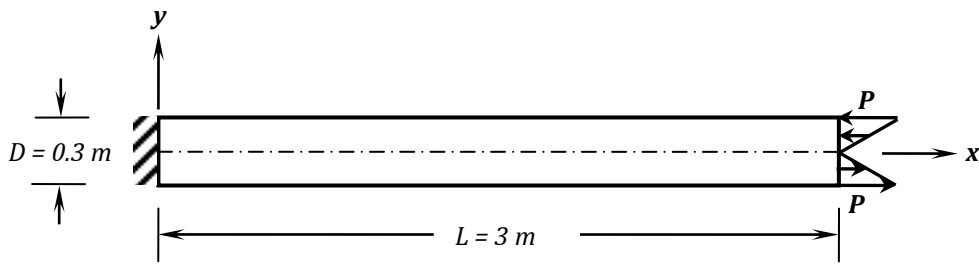


Figure 8: Cantilever under pure bending

Table (4): Average Nodal Stress in x-direction at mid span

LOAD (N)	Stress (N/mm ²)			
	Log	Green	Eng (Geom)	Eng Exact
0	0	0	0	0
6000	1.24E+00	1.22E+00	1.24E+00	1.23E+00
12000	2.50E+00	2.41E+00	2.47E+00	2.43E+00
18000	3.58E+00	3.49E+00	3.54E+00	3.37E+00
24000	3.94E+00	4.35E+00	4.09E+00	3.63E+00
30000	2.71E+00	4.84E+00	3.58E+00	2.61E+00

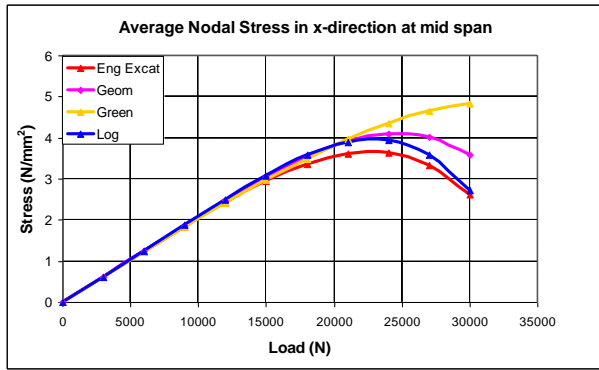


Fig. (9): Average Nodal Stress in x-direction at mid span

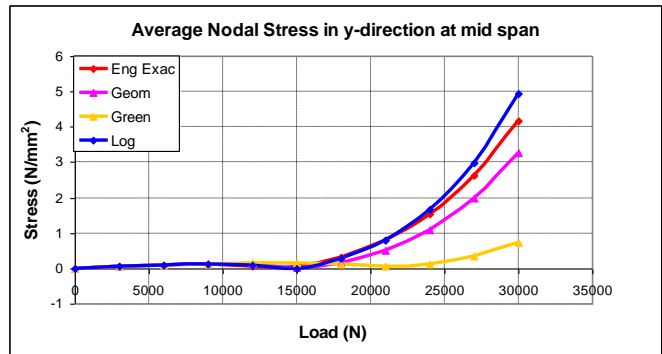


Fig. (10): Average Nodal Stress in y-direction at mid span

Table (5): Average Nodal Stress in y-direction at mid span

LOAD (N)	Stress (N/mm ²)			
	Log	Green	Eng (Geom)	Eng Exact
0	0	0	0	0
6000	9.62E-02	9.75E-02	9.59E-02	9.13E-02
12000	1.05E-01	1.66E-01	1.21E-01	7.57E-02
18000	2.86E-01	1.33E-01	1.50E-01	3.18E-01
24000	1.67E+00	1.15E-01	1.10E+00	1.54E+00
30000	4.92E+00	7.18E-01	3.26E+00	4.18E+00

Table (6): Average Shear Stress at mid span

LOAD (N)	Stress (N/mm ²)			
	Log	Green	Eng (Geom)	Eng Exact
0	0	0	0	0
6000	4.47E-05	6.77E-04	1.26E-03	2.67E-03
12000	1.50E-02	5.56E-03	1.48E-02	2.23E-02
18000	8.82E-02	2.32E-02	6.87E-02	8.97E-02
24000	2.83E-01	6.56E-02	2.02E-01	2.48E-01
30000	6.39E-01	1.47E-01	4.43E-01	5.40E-01

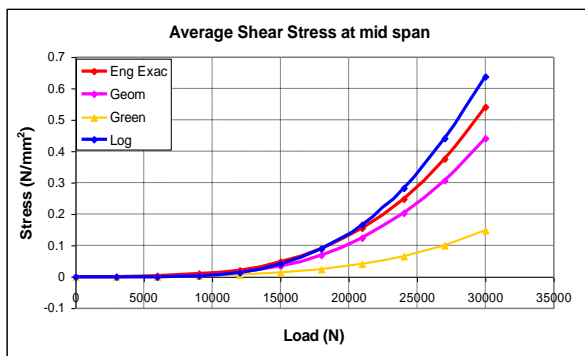


Fig. (11) Average shear stress at mid-span

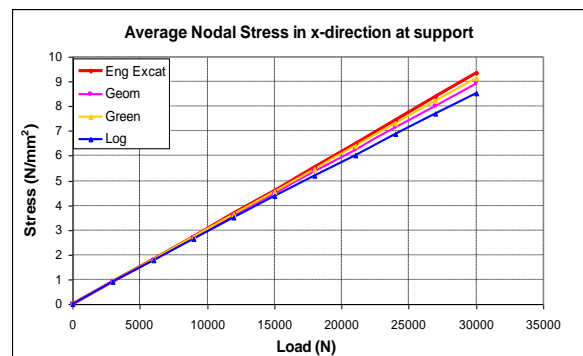


Fig. (12) Average Nodal Stress in x-direction at support

Table (7): Average Nodal Stress in x-direction at support

LOAD (N)	Stress (N/mm ²)			
	Log	Green	Eng (Geom)	Eng Exact
0	0	0	0	0
6000	1.78E+00	1.81E+00	1.80E+00	1.82E+00
12000	3.50E+00	3.64E+00	3.58E+00	3.66E+00
18000	5.19E+00	5.47E+00	5.35E+00	5.54E+00
24000	6.86E+00	7.31E+00	7.12E+00	7.44E+00
30000	8.52E+00	9.15E+00	8.90E+00	9.36E+00

Table (8): Average Nodal Stress in y direction at support

LOAD (N)	Stress (N/mm ²)			
	Log	Green	Eng (Geom)	Eng Exact
0	0	0	0	0
6000	9.62E-02	9.75E-02	9.59E-02	9.13E-02
12000	1.05E-01	1.66E-01	1.21E-01	7.57E-02
18000	2.86E-01	1.33E-01	1.50E-01	3.18E-01
24000	1.67E+00	1.15E-01	1.10E+00	1.54E+00
30000	4.92E+00	7.18E-01	3.26E+00	4.18E+00

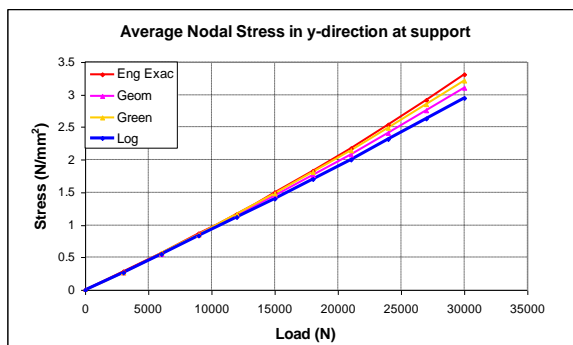


Fig. (13): Average Nodal Stress in y-direction at support

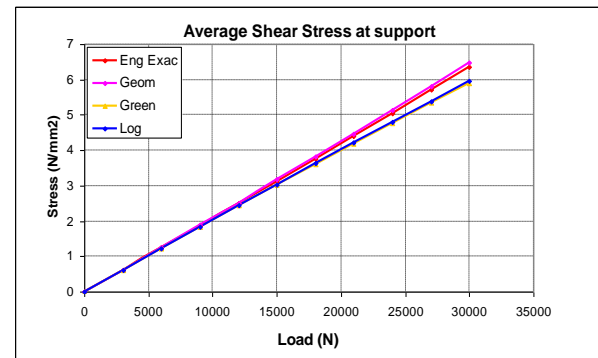


Fig. (14): Average Shear Stress at support

Table (9): Average Shear Stress at support

LOAD (N)	Stress (N/mm ²)			
	Log	Green	Eng (Geom)	Eng Exact
0	0	0	0	0
6000	1.23E+00	1.23E+00	1.25E+00	1.24E+00
12000	2.44E+00	2.43E+00	2.52E+00	2.50E+00
18000	3.64E+00	3.61E+00	3.82E+00	3.77E+00
24000	4.81E+00	4.77E+00	5.14E+00	5.05E+00
30000	5.97E+00	5.90E+00	6.49E+00	6.36E+00

3.3 Clamped beam under point force

A beam with two-fixed ends is considered. The beam is of length $L = 200 \text{ mm}$, height $D = 10 \text{ mm}$ and thickness 1 mm as shown in Figure (15). The numerical values for material property parameters are Young's modulus, $E = 210 \text{ GPa}$, Poisson's ratio, $\nu = 0.3$. The beam is modeled with a mesh of 20-elements.

The variation of the stresses at the support and at mid-span with the load increments as computed from the Eng Exact formulation and for the approximate Eng and Green formulations (Ref. [15]), are compared with the true stresses(Ref. [17]) in Figures (16) to (21).

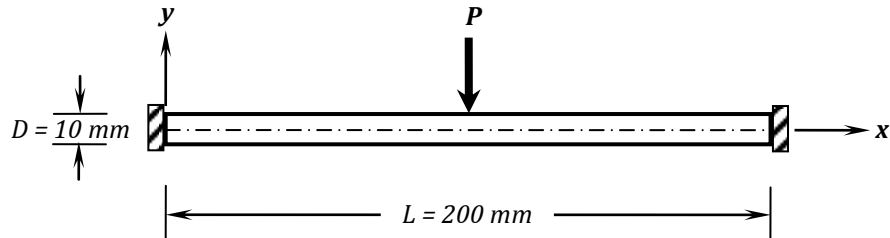


Fig. (15): Clamped beam under point force

Tables (10), (11) and (12) show the values for average nodal stresses at mid-span. Very large loads were applied in example resulting in large strains.

There is a marked difference between the Green and the other formulations' values for the stresses at the support for large load values. This is expected for cases of large strain. The Eng Exact values are the closest to the Log (Cauchy) values for direct stresses. A similar trend is shown by the values of the stresses in the x-direction at mid span with a maximum percentage difference between the Eng Exact and Log values of about 7% (around 69% for the Green and 37% for Eng). The stress at mid-span in the y-direction shows a similar variation with the Eng Exact and Log values in close agreement and continuously increasing and the Green values almost constant and close to zero. The maximum difference between the Eng Exact values and Eng values is around 45%. This clearly shows the effect of assuming that the shear strain is small. The Eng Exact shear stresses at mid-span values are large, compared to the other values, and are almost of a linear variation. The Log and Eng shear values are in close agreement. This results from the assumption that the shear strain is small in these formulations. The Green shear values at mid-span are very small compared to the values from the other formulations and are of a non- uniform alternating nature. Thus, the Green strain formulation is not suitable for evaluating the correct physical stresses. Also, the assumption that the shear strain is small limits the use of the approximate Eng formulation for cases of small strain. Table (13) and Figure (22) show the maximum principal stresses at mid-span for the Log and Eng Exact formulations. These are almost identical with a maximum difference of about 6%. Hence, the stresses obtained using the Eng Exact formulation are considered to be the correct measure of the physical stresses in large strain GNL.

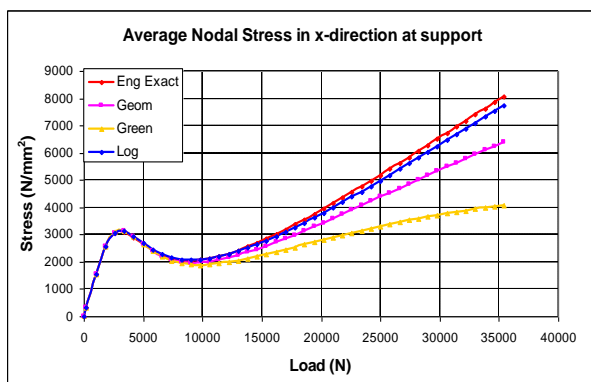


Fig. (16): Average Nodal Stress in x-direction at support

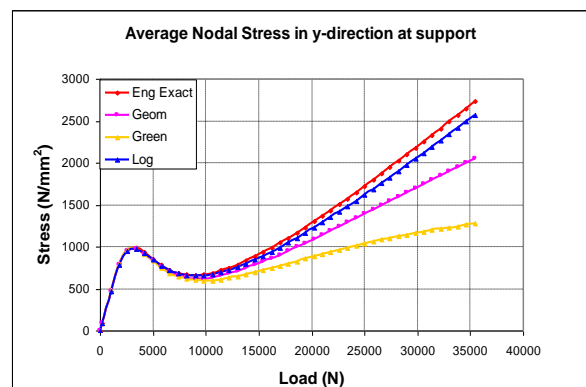


Fig. (17): Average Nodal Stress in y-direction at support

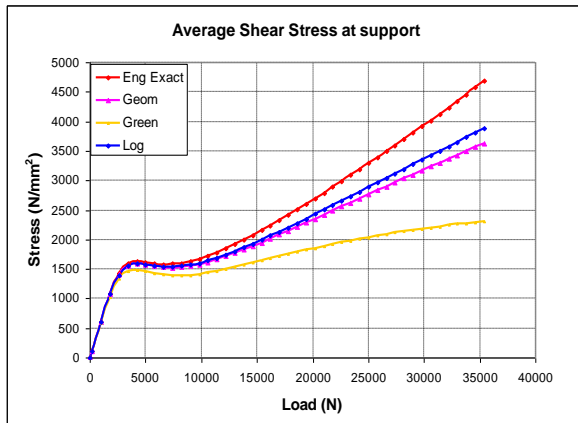


Fig. (18): Average Shear Stress at support

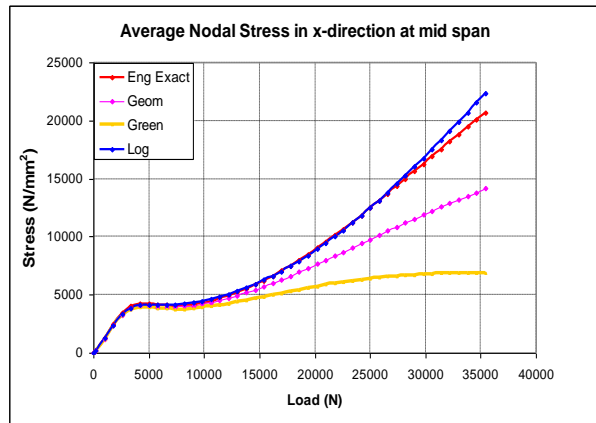


Fig. (19): Average Nodal Stress in x-direction at mid span

Table (10): Average Nodal Stress in x-direction at mid span

LOAD (N)	Stress (N/mm ²)				LOAD (N)	Stress (N/mm ²)			
	Log	Green	Eng (Geom)	Eng Exact		Log	Green	Eng (Geom)	Eng Exact
0	0	0	0	0	17800	7.47E+03	5.31E+03	6.64E+03	7.52E+03
1000	1.25E+03	1.23E+03	1.23E+03	1.23E+03	19400	8.40E+03	5.60E+03	7.30E+03	8.50E+03
2600	3.46E+03	3.28E+03	3.26E+03	3.31E+03	21000	9.44E+03	5.86E+03	7.98E+03	9.55E+03
4200	4.23E+03	4.00E+03	3.92E+03	4.10E+03	22600	1.06E+04	6.10E+03	8.69E+03	1.07E+04
5800	4.15E+03	3.98E+03	3.84E+03	4.13E+03	24200	1.18E+04	6.30E+03	9.41E+03	1.19E+04
7400	4.07E+03	3.95E+03	3.77E+03	4.14E+03	25800	1.31E+04	6.48E+03	1.01E+04	1.31E+04
9000	4.18E+03	4.07E+03	3.83E+03	4.29E+03	27400	1.45E+04	6.62E+03	1.08E+04	1.43E+04
10600	4.47E+03	4.34E+03	4.01E+03	4.59E+03	29000	1.60E+04	6.74E+03	1.15E+04	1.56E+04
12200	4.93E+03	4.71E+03	4.26E+03	5.03E+03	30600	1.75E+04	6.82E+03	1.22E+04	1.69E+04
13800	5.52E+03	5.18E+03	4.55E+03	5.59E+03	32200	1.91E+04	6.88E+03	1.29E+04	1.82E+04
15400	6.24E+03	5.72E+03	4.86E+03	6.26E+03	33800	2.07E+04	6.92E+03	1.35E+04	1.95E+04
17000	7.07E+03	6.32E+03	5.16E+03	7.04E+03	35400	2.23E+04	6.93E+03	1.41E+04	2.07E+04

Table (11): Average Nodal Stress in y-direction at mid span

LOAD (N)	Stress (N/mm ²)				LOAD (N)	Stress (N/mm ²)			
	Log	Green	Eng (Geom)	Eng Exact		Log	Green	Eng (Geom)	Eng Exact
0	0	0	0	0	17800	1.76E+03	6.18E+02	1.57E+03	2.20E+03
1000	3.21E+02	3.17E+02	3.21E+02	3.39E+02	19400	2.35E+03	7.55E+02	2.01E+03	2.90E+03
2600	7.52E+02	7.14E+02	7.41E+02	8.76E+02	21000	3.03E+03	8.75E+02	2.48E+03	3.68E+03
4200	6.43E+02	5.45E+02	6.08E+02	7.71E+02	22600	3.80E+03	9.77E+02	2.97E+03	4.54E+03
5800	3.39E+02	2.13E+02	2.97E+02	3.94E+02	24200	4.65E+03	1.06E+03	3.48E+03	5.45E+03
7400	1.52E+02	1.93E+01	1.20E+02	1.58E+02	25800	5.58E+03	1.12E+03	4.00E+03	6.41E+03
9000	1.13E+02	2.03E+01	9.79E+01	1.10E+02	27400	6.58E+03	1.15E+03	4.51E+03	7.40E+03
10600	1.98E+02	1.07E+01	1.98E+02	2.23E+02	29000	7.65E+03	1.17E+03	5.03E+03	8.43E+03
12200	3.87E+02	1.13E+02	3.92E+02	4.69E+02	30600	8.77E+03	1.17E+03	5.54E+03	9.47E+03
13800	6.69E+02	2.47E+02	6.60E+02	8.33E+02	32200	9.93E+03	1.15E+03	6.03E+03	1.05E+04
15400	1.04E+03	3.95E+02	9.89E+02	1.30E+03	33800	1.11E+04	1.11E+03	6.50E+03	1.16E+04
17000	1.50E+03	5.45E+02	1.37E+03	1.88E+03	35400	1.23E+04	1.06E+03	6.96E+03	1.26E+04

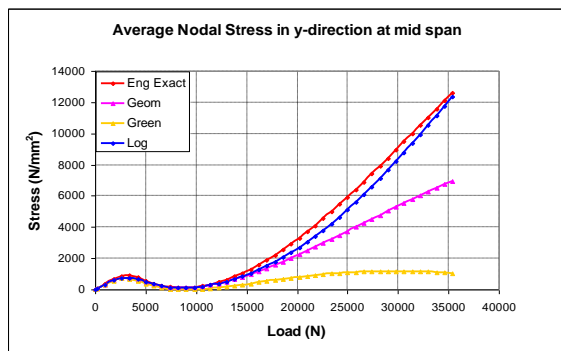


Fig. (20): Average Nodal Stress in y-direction at mid span

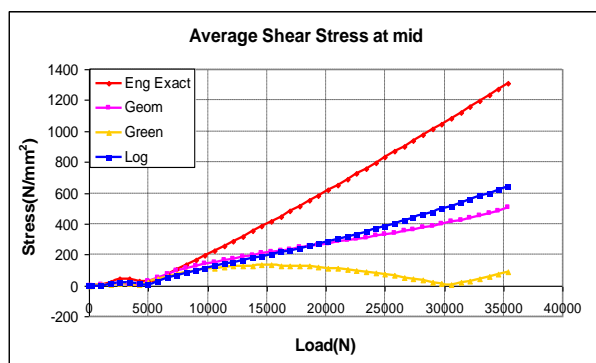


Fig. (21): Average Shear Stress at mid span

Table (12): Average Shear Stress at mid span

LOAD (N)	Stress (N/mm ²)				LOAD (N)	Stress (N/mm ²)			
	Log	Green	Eng (Geom)	Eng Exact		Log	Green	Eng (Geom)	Eng Exact
0	0	0	0	0	17800	2.42E+02	1.26E+02	2.45E+02	5.14E+02
1000	3.73E-01	1.12E+00	1.43E+00	1.87E+00	19400	2.70E+02	1.18E+02	2.63E+02	5.82E+02
2600	2.11E+01	1.31E+01	1.07E+01	3.90E+01	21000	3.01E+02	1.08E+02	2.82E+02	6.52E+02
4200	1.12E+01	2.21E+00	8.19E+00	2.74E+01	22600	3.33E+02	9.55E+01	3.01E+02	7.23E+02
5800	2.74E+01	4.11E+01	5.19E+01	3.50E+01	24200	3.66E+02	8.01E+01	3.21E+02	7.94E+02
7400	6.55E+01	7.47E+01	9.21E+01	1.03E+02	25800	4.02E+02	6.24E+01	3.42E+02	8.66E+02
9000	9.75E+01	9.85E+01	1.25E+02	1.66E+02	27400	4.38E+02	4.24E+01	3.63E+02	9.38E+02
10600	1.25E+02	1.14E+02	1.52E+02	2.27E+02	29000	4.76E+02	2.04E+01	3.87E+02	1.01E+03
12200	1.51E+02	1.24E+02	1.75E+02	2.88E+02	30600	5.16E+02	3.49E+00	4.12E+02	1.08E+03
13800	1.76E+02	1.29E+02	1.96E+02	3.50E+02	32200	5.57E+02	2.92E+01	4.40E+02	1.16E+03
15400	2.01E+02	1.31E+02	2.16E+02	4.14E+02	33800	5.99E+02	5.66E+01	4.70E+02	1.23E+03
17000	2.28E+02	1.28E+02	2.35E+02	4.80E+02	35400	6.43E+02	8.55E+01	5.02E+02	1.31E+03

Table (13) Maximum Principal Stress at Mid-span

LOAD (N)	Stress (N/mm ²)		LOAD	Stress (N/mm ²)		LOAD (N)	Stress (N/mm ²)	
	Log	Eng Exact		Log	Eng Exact		Log	Eng Exact
0	0.0	0.0	12200	4935.0	5048.0	24200	11819.0	11996.0
1000	1250.0	1230.0	13800	5526.0	5616.0	25800	13121.0	13210.0
2600	3460.0	3311.0	15400	6248.0	6294.0	27400	14524.0	14425.0
4200	4230.0	4100.0	17000	7079.0	7084.0	29000	16027.0	15740.0
5800	4150.0	4130.0	18600	7931.0	8054.0	30600	17530.0	17054.0
7400	4071.0	4143.0	20200	8923.0	9076.0	32200	19134.0	18371.0
9000	4182.0	4297.0	21800	10015.0	10178.0	33800	20737.0	19687.0
10600	4474.0	4602.0	23400	11217.0	11390.0	35400	22341.0	20907.0

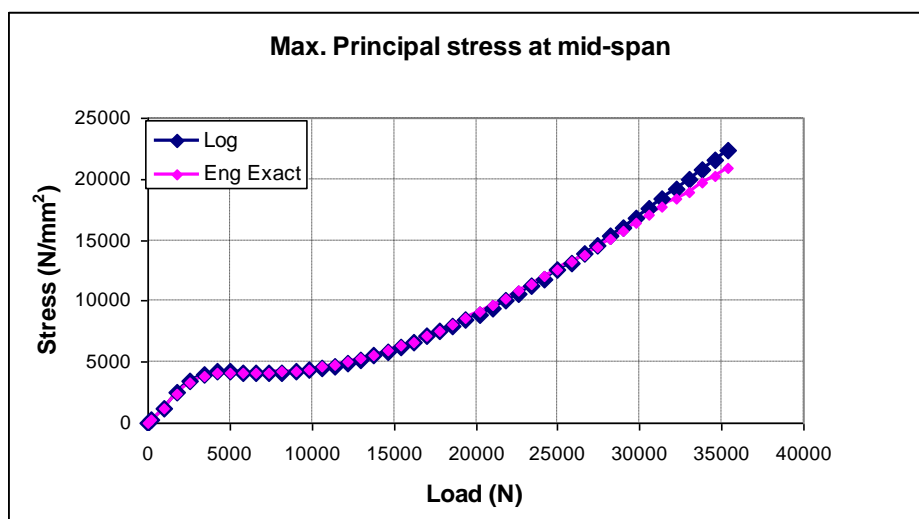


Fig. (22) Maximum Principal Stress at Mid-span

IV. CONCLUSIONS

Based on the results of the numerical examples, it can be concluded that:

1. The Total Lagrangian solutions based on the Green strains and 2nd Piola-Kirchhoff stresses while being not suitable for evaluating the correct physical stresses are necessary for use as a base for the solutions based on Engineering stresses.
2. The exact Engineering strain based formulation results in correct physical stresses, which are very close to the true Cauchy stresses especially for small and moderately large strains. Bearing in mind the fact that the elastic constants are evaluated using these stresses, these formulations must be used when stresses are required in a Total Lagrangian analysis.
3. The formulation based on approximate Engineering strains give excellent results in structures wherein the shear strains are small.

4. The use of Logarithmic strains is necessary when the exact true stresses are required. The results from the Log formulation presented here can be further enhanced by removing the restriction of small shear strains.
5. The formulation based on the exact Engineering strains can be easily extended to three-dimensional analysis.

REFERENCES

- [1] Yang, Y. B. and Kuo, S. R., Theory and Analysis of Nonlinear Framed Structures, Prentice Hall, Simon & Schuster (Asia), 1998, Singapore.
- [2] Crisfield, M. A., Non-linear Finite Element Analysis of Solids and Structures, Volume 1, John Wiley & Sons Ltd., August 1997, Chichester, England.
- [3] Zienkiewicz O. C. and Taylor, R. L., The Finite Element Method for Solids and Structural Mechanics, 6th edition , Butterworth Heinemann 2005, Elsevier.
- [4] Mohamed, A. E., A Small Strain Large Rotation Theory and Finite Element Formulation of Thin Curved Beams, Ph.D. Thesis, 1983, The City University, London.
- [5] Belytschko, T., Finite Elements for Nonlinear Continua & Structures, North-Westren University, 1998, Evanston.
- [6] Marinkovic`, D., Koppe, H. and Gabbert, U., Degenerated shell element for geometrically nonlinear analysis of thin-walled piezoelectric active structures, Smart Mater. Struct. 17, 2008, 015030 (10pp), IOP Publications, G.B.
- [7] Wood, R. D. and Zienkiewicz, O. C., Geometrically Nonlinear Finite Element Analysis of Beams, Frames, Arches and Axisymmetric Shells, Computers & Structures, 1977, Vol.7, pp 725-735, PergamonPress, G.B.
- [8] Surana, K. S. and Sorem, R. M., Geometrically Nonlinear Formulation for Three Dimensional Curved Beam Elements with Large Rotations, Int. J. Num. Meth. Engng., 1989, Vol.28, 43-73.
- [9] Djermane, M., Chelghoum, A. ,Amieur, B. and Labbaci, B., Linear and Nonlinear Thin Shell Analysis using a Mixed Finite with Drilling Degrees of Freedom, Int. J. Applied Engng. Research, 2006, Vol. 1 No. (2) pp 217-236.
- [10] Bonet, J. and Wood, R.D., Nonlinear Continuum Mechanics for Finite Element Analysis, CambridgeUniversity Press, 1997, Cambridge, U.K.
- [11] Mohamed, A. E. and Adam, F. M., Large Deformation Finite Element Analysis of Shell Structures, Journal of Science & Technology, June 2003, Vol.4-No. 2, 47-58, SUST, Khartoum, Sudan.
- [12] Adam, F. M. and Elzubair, A., Large Deformation Finite Element Analysis of Shells, Degenerated Eight Nodes Shell Element, LAP LAMBERT Academic Publishing, 2012, Germany.
- [13] Akasha Hilal, N. M., Development of Geometrically Nonlinear Finite Element Program using Plane Stress/Strain Elements based on Engineering and True Stress Measures, Ph. D. Thesis, SUST, October 2009, Khartoum, Sudan.
- [14] Akasha, N. M. and Mohamed, A. E., Geometrically Nonlinear Analysis using Plane Stress/Strain Elements based on Alternative Strain Measures”, Journal of Science & Technology; Engng. Comp. Sciences, June 2012, Vol. 13- No. 1- 1-12, SUST, Khartoum, Sudan.
- [15] Akasha, N. M. and Mohamed, A. E., Evaluation of Engineering Stress for Geometrically Nonlinear Plane Stress/Strain Problems, JASER, June 2012, Vol. 2, No. 2, , 115-125, Design for Scientific Renaissance.
- [16] Greco, M. and Ferreira, I. P., Logarithmic strain measure applied to the nonlinear formulation for space truss analysis, Finite Elements in Analysis and Design, 2009, 45, 632-639.
- [17] Akasha, N. M. and Mohamed, A. E., Evaluation of True Stress for Geometrically Nonlinear Plane Stress/Strain Problems, JASER, March 2012, Vol.2, No.1, 68-79, Design for Scientific Renaissance.